中文 English

主页
征文通知
会议组织
论文投稿
会议注册及终稿
会议程序
大会报告
大会专题研讨会
会前专题讲座
关肇直奖
张贴论文奖
会场、酒店与交通
旅游

第35届中国控制会议（CCC2016）欢迎您！

第35届中国控制会议（CCC2016）将于2016年7月27-29日在四川成都举办。中国控制会议由中国自动化学会控制理论专业委员会（TCCT）发起，现已成为控制理论与技术领域的国际性学术会议。会议旨在为系统、控制及其自动化领域的国内外学者与技术人员提供一个学术交流平台，展示最新的理论与技术成果。会议采用大会报告、专题研讨会、会前专题讲座、分组报告和张贴论文等形式进行交流。会议的工作语言为中文和英文。自2006年起会议论文集进入IEEE Xplore，并由EI收录。

成都，天府之国，如诗如画，是一个时尚与古风氤氲交融、生气盎然的城市。您可于翠竹清溪间品茗论道，亦可寻找散落于大街小巷的美食美景，还可在会议之余游历川中名胜，探访藏区羌寨。古城蕴容，学坛论道，2016年的成都定会令您不虚此行！

总主席
郭　雷
中国科学院

总主席
周克敏
西南交通大学

副总主席
冯晓云
西南交通大学

主办单位

承办单位

协办单位

投稿网站
http://cms.amss.ac.cn

重要日期

提交论文初稿截至日期
2016年3月1日

论文录用通知日期
2016年4月1日

提交论文终稿截至日期
2016年5月20日

最新消息

第35届中国控制会议投稿声明
2015-10-31

第35届中国控制会议论文集已被EI Compendex检···
2016-12-01

第35届中国控制会议论文集已进入IEEE Xplore...
2016-09-05

关于CCC2016会场周边交通管制的重要提醒
2016-07-08

联系方式

程序委员会秘书处：
曲莹（女士）
北京中关村东路55号中国科学院数学与系统科学研究院（邮编：100190）
+86-10-82541403
ccc@amss.ac.cn

组织委员会秘书处：
秦娜（女士）
四川省成都市二环路北一段111号西南交通大学电气工程学院（邮编：610031）
+86-13540067894
ccc2016@my.swjtu.edu.cn

Co-Chair: Pan, Lin — Wuhan Univ. of Tech.

ThA09-1 13:30--13:50

Iterative Learning Control Based Phase Splits Strategy for Oversaturated Urban Traffic Network

Jin, Shangtai — Beijing Jiaotong Univ.
Hou, Zhongsheng — Beijing Jiaotong Univ.
Chi, Ronghu — Qingdao Univ. of Sci. & Tech.
Wang, Danwei — Nanyang Technological Univ.
Bu, Xuhui — Henan Polytechnic Univ.

ThA09-2 13:50--14:10

Downsampled shift Repetitive Control for PWM DC/AC Converters

Xu, Guofeng — Nanjing Univ. of Aeronautics & Astronautics
Ye, Yongqiang — Nanjing Univ. of Aeronautics & Astronautics
Qian, Shuqu — Anshun Univ.
Zhu, Mingzhe — Nanjing Univ. of Aeronautics & Astronautics

ThA09-3 14:10--14:30

Dynamic Modularity Approach to Adaptive Inner/Outer Loop Control of Robotic Systems

Wang, Hanlei — Beijing Inst. of Control Engineering
Ren, Wei — Univ. of California, Riverside
Cheah, Chien Chern — Nanyang Technological Univ.
Xie, Yongchun — Beijing Inst. of Control Engineering

ThA09-4 14:30--14:50

LPV-MRAC Method for Aircraft with Structural Damage

Peng, Bo — Beihang Univ.
Yang, Lingyu — beihang Univ.
Yang, Xiaoke — Beihang Univ.

ThA09-5 14:50--15:10

Consolidated Iterative Learning Control and A Preliminary Case Study

Cai, Yangguang — Beihang Univ.
Wei, Zi-Bo — Beihang Univ.
Quan, Quan — Beihang Univ.

ThA09-6 15:10--15:30

Composite Learning: An Efficient Way of Parameter Estimation in Adaptive Control

Pan, Yongping — National Univ. of Singapore
Pan, Lin — Wuhan Univ. of Tech.
Darouach, Mohamed — Univ. of Lorraine, IUT of Longwy
Yu, Haoyong — National Univ. of Singapore

ThA10, 13:30--15:30 A7

Regular English Session: Hybrid Systems and Discrete Event Dynamic Systems

Chair: Qi, Yiwen — Shenyang Aerospace Univ.

Co-Chair: Li, Liang — The No.719 Research Inst. of CSIC

ThA10-1 13:30--13:50

LMI-based Stabilization for Switched Linear Systems With Event-triggering Scheme

Zeng, Pengyu — Shenyang Aerospace Univ.
Qi, Yiwen — Shenyang Aerospace Univ.

ThA10-2 13:50--14:10

Observer-based reset law design for linear uncertain systems based on model predictive strategy

Mi, Jie — Taiyuan Univ. of Tech.
Zhao, Guanglei — Yanshan Univ.

ThA10-3 14:10--14:30

Periodically intermittent H_∞ control for a class of nonlinear systems

Liu, Lijun — Guangxi Univ.
Chen, Wu-Hua — Guangxi Univ.

Proceedings of the 35th Chinese Control Conference
July 27-29, 2016, Chengdu, China

LPV-MRAC Method for Aircraft with Structural Damage

Peng Bo[1], Yang Lingyu[1], Yang Xiaoke[1]
1. Beihang University, Beijing 100190, P. R. China
E-mail: nake_peng@163.com, yanglingyu@buaa.edu.cn, das.xiaoke@hotmail.com

Abstract: Abrupt structural damage poses significant challenges to the flight safety and flight quality of aircraft. In this paper, a direct model reference adaptive control (MRAC) method based on a linear parameter-varying (LPV) model is proposed to recover the control performance and flight quality of damaged aircraft. The design of the controller is based on a polytopic LPV model and the higher order singular value decomposition (HOSVD) model reduction method to reduce the computational cost of identifying the damaged aircraft model. The proposed controller also extends a previous MRAC method which assumes the input matrix is unchanged for different damage cases by identifying an uncertain input parameter online. The developed LPV-MRAC method is validated by simulation on NASA's generic transport model (GTM) with left wing tip loss damage and shown to be capable of compensating the damage effects and restoring the aircraft's control performance shortly after the damage. The flight quality of the closed-loop damaged aircraft is also evaluated by the C-star criterion and shown to be within Class I under the proposed controller.

Key Words: Model reference adaptive control, Aircraft with structural damage, Uncertainty of input matrix, Polytopic LPV models

1 Introduction

Modern aircraft, despite advanced instrumentation and various fault-tolerant designs, face abrupt structural damage like wing tip break up [1] or vertical-tail loss [2] at times. It has been shown that abrupt structural damage to airframe and engines, which can result in considerable deterioration in flight performance and aircraft handling quality, has led to quite a few aircraft accidents [3]. Nowadays, to recover flight performance and aircraft handling quality has drawn researchers' effort in related fields, and lots of studies have been conducted.

The team of Tao proposes a multivariable adaptive control algorithm, which is based on a nonlinear aircraft model, and applies it to the simulation of a genetic transport model (GTM) form NASA [1]. Nguyen proposes a hybrid adaptive control scheme with artificial neural networks, which contains pre-trained and on-line learning networks, and design a controller design is based on the nonlinear model of the GTM [4, 5]. Santillo uses a control scheme named Retrospective-Cost Adaptive Control and demonstrates it to the GTM model successfully under vertical gust disturbance[6]. The team of Hovakimyan proposes an $\mathcal{L}_1$ adaptive control algorithm [7, 8] and applies it in the flight test of the GTM[9]. Yucelen uses a Derivative-Free MRAC algorithm to simulate on the nonlinear model of an aircraft with abrupt structural damage[10].

The methods above use either linear or nonlinear models to design control and adaptive laws, while Xu adopts an MRAC control method with a polytopic LPV model to deal with the uncertainties of structural and parametric changes caused by abrupt structural damage [11]. In [11], Xu models the damaged aircraft with polytopic LPV models to design control laws and adaptive laws. The method is also demonstrated to be effective, i.e. the controlled states converge to stable values and the error asymptotically convergence to zero. However, it assumes in [11] that the input matrix $\mathbf{B}$ remains unchanged under different damage cases, which simplifies the design but restricts its applicability. So in this paper, we propose a direct MRAC scheme, which inherits the polytopic LPV model in [11] to speed up the convergence of adaptive parameters by reducing the computational cost of identifying the damaged model. Further more, the uncertainty of input matrix is explicitly considered by a matrix column transformation to improve the applicability of the proposed LPV-MRAC method.

The rest of this paper is organized as follows. Section 2 discusses the LPV model of aircraft with abrupt structural damage in detail. Section 3 covers the design of control laws and adaptive laws of the proposed LPV-MRAC method. A case study on the GTM with left wing tip loss is carried out in Section 4. White Gaussian measurement noises are added to the aircraft states and simulation results are also analysed therein. Furthermore, aircraft handling quality is evaluated and compared before and after damage. Section 5 summaries the LPV-MRAC method and proposes future research directions.

2 LPV Modelling of Structural Damaged Aircraft

2.1 Polytopic LPV Models

The dynamics of aircraft with structural damage can be modelled by a general nonlinear ordinary differential equation as

$$\dot{\mathbf{x}}_n = \mathbf{f}(\mathbf{x}_n, \mathbf{u}_n, \mathbf{p}), \tag{1}$$

where $\mathbf{x}_n \in \mathbb{R}^n$, $\mathbf{u}_n \in \mathbb{R}^m$ are the state and input vector, respectively, and $\mathbf{p} \in \mathbb{R}^l$ is a damage severity vector for the l types of damage cases. (1) can be linearised around the given operating point $(\mathbf{x}_{n0}, \mathbf{u}_{n0})$, leading to a linear state-space description with $\mathbf{p}$ as,

$$\Delta\dot{\mathbf{x}}_n = \mathbf{A}(\mathbf{p})\Delta\mathbf{x}_n + \mathbf{B}(\mathbf{p})\Delta\mathbf{u}_n + \mathbf{f}_0(\mathbf{p}), \tag{2}$$

where $\Delta\mathbf{x}_n = \mathbf{x}_n - \mathbf{x}_{n0}$, $\Delta\mathbf{u}_n = \mathbf{u}_n - \mathbf{u}_{n0}$, $\mathbf{A}(\mathbf{p}) = \frac{\partial \mathbf{f}(\mathbf{x}_n,\mathbf{u}_n,\mathbf{p})}{\partial \mathbf{x}_n}|_{(\mathbf{x}_{n0},\mathbf{u}_{n0})}$, and $\mathbf{B}(\mathbf{p}) = \frac{\partial \mathbf{f}(\mathbf{x}_n,\mathbf{u}_n,\mathbf{p})}{\partial \mathbf{u}_n}|_{(\mathbf{x}_{n0},\mathbf{u}_{n0})}$. Because an operating point is not the trim point in general, an offset term $\mathbf{f}_0(\mathbf{p}) = \mathbf{f}(\mathbf{x}_{n0}, \mathbf{u}_{n0}, \mathbf{p})$ is added to the state-space equation (2). Since $\mathbf{A}(\mathbf{p})$, $\mathbf{B}(\mathbf{p})$ and $\mathbf{f}_0(\mathbf{p})$ are time-varying functions of the $\mathbf{p}$, (2) is a typical linear parameter-varying system and can be approximated by the following

This research is funded by National Natural Science Foundation (NNSF) of China (Grant no.61273099).

polytopic form

$$\Delta\dot{\mathbf{x}}_n = \sum_{i=1}^{k} \boldsymbol{\alpha}_i(\mathbf{p})\mathbf{A}_i^*\Delta\mathbf{x}_n + \sum_{i=1}^{k} \boldsymbol{\alpha}_i(\mathbf{p})\mathbf{B}_i^*\Delta\mathbf{u}_n + \mathbf{f}_0(\mathbf{p}), \tag{3}$$

where $[\mathbf{A}(\mathbf{p}), \mathbf{B}(\mathbf{p})] \in \Omega \triangleq \mathrm{Co}\{[\mathbf{A}_1^*, \mathbf{B}_1^*], \ldots, [\mathbf{A}_k^*, \mathbf{B}_k^*]\}$, k is the number of polytopic vertexes, $[\mathbf{A}_i^*, \mathbf{B}_i^*]$ are some known matrices, and $\mathrm{Co}\{\ldots\}$ denotes the convex hull. $\boldsymbol{\alpha}_i(\mathbf{p})$ is the interpolation coefficient which satisfies the following conditions,

$$\sum_{i=1}^{k} \boldsymbol{\alpha}_i(\mathbf{p}) = 1, \;\; 0 \leqslant \boldsymbol{\alpha}_i(\mathbf{p}) \leqslant 1. \tag{4}$$

The interpolation coefficient $\boldsymbol{\alpha}_i(\mathbf{p})$ and the offset term $\mathbf{f}_0(\mathbf{p})$ change with the damage severities, therefore the adaptive algorithm only needs to identify $\boldsymbol{\alpha}_i(\mathbf{p})$ and $\mathbf{f}_0(\mathbf{p})$ to obtain the model of the damaged aircraft.

Note in literature, the T-S fuzzy model [12] is similar to the expressions in (3) (4), but the physical meaning of the parameters and the relevant derivations are distinct.

2.2 Model Reduction through HOSVD

To avoid excessive computational load introduced by a fine grid, the higher order singular value decomposition (HOSVD) in [13] is used to reduce the number of polytopic vertexes without reducing much accuracy. As the matrix singular value decomposition (SVD) explores the correlation between the two dimensions of the matrix and decomposes the matrix into some orthogonal bases and corresponding singular values, the HOSVD extends this idea to higher dimensional arrays or tensors, and explores the correlation between those additional dimensions. In order to apply the HOSVD to get the LPV model in (3), we first discretize the parameter space and stack the model on each node in a Tensor Product (TP) form, then calculate the singular values through HOSVD. The smaller singular values are discarded to reduce the number of vertexes.

Firstly, in the range of damage concerned, a grid is generated for the vector $\mathbf{p}$. Each node of the grid represents a case of damage. The nonlinear aircraft model is linearized at each node, leading to the following linearised model,

$$\mathbf{S}_{i_1 i_2 \ldots i_l} = \left[\; \mathbf{A}_{i_1 i_2 \ldots i_l} \quad \mathbf{B}_{i_1 i_2 \ldots i_l} \;\right], \tag{5}$$

where $i_1, \ldots, i_l$ denotes the indices of the nodes in each dimension of the grid and $i_1 = \{1, \ldots, I_1\}, \ldots, i_l = \{1, \ldots, I_l\}$. $I_1, \ldots, I_l$ denote the number of grid points in each dimension of the grid. Then the resulting model is described in a TP form through a n-mode matrix-tensor product form [13] as

$$\mathbf{S}(\mathbf{p}) = \mathcal{S} \bigotimes_{i=1}^{l} \boldsymbol{\omega}_i(\mathbf{p}), i \in \{1, 2, \ldots l\}, \tag{6}$$

where $\mathcal{S} \in \mathbb{R}^{I_1 \times I_2 \times \ldots I_l \times m \times (m+n)}$ is a tensor constructed from the system matrix (5). $\bigotimes_{i=1}^{l}$ denotes the successive i-mode matrix-tensor product. $\boldsymbol{\omega}_i(\mathbf{p}) \in \mathbb{R}^{I_i}$ denotes the weight for each model in the i^{th} dimension of the grid. At last, the HOSVD method is applied to calculate the singular values of the TP form to simplify the gird. By omitting the smaller singular values, the number of models and interpolation coefficients can be reduced without losing much accuracy as compared with the original one. Using this method, the TP model can be approximated by

$$\mathbf{S}(\mathbf{p}) = \mathcal{S} \bigotimes_{i=1}^{l} \boldsymbol{\omega}_i(\mathbf{p}) \approx \mathcal{S}^* \bigotimes_{i=1}^{l} \boldsymbol{\omega}_i^*(\mathbf{p}), \tag{7}$$

where $\mathcal{S}^*$ and $\boldsymbol{\omega}_i^*(\mathbf{p})$ are the tensor and the weight vector of the reduced order system respectively, and $\boldsymbol{\omega}_i^*(\mathbf{p}) \in \mathbb{R}^{J_i}$ with $J_i << I_i$.

2.3 Simplified Model of the GTM

In this section, we use the above HOSVD method to obtain a simplified model of the GTM.

Assume that the polytopic model of the GTM can be written as in (2), where $\mathbf{x}_n \triangleq [q \quad p \quad r \quad v \quad \alpha \quad \beta]^T$ is the state vector. It can be rewitten as $\mathbf{x}_n = [\mathbf{x}^T \quad \mathbf{z}^T]^T$, where $\mathbf{x} \triangleq [q \quad p \quad r]^T$ and $\mathbf{z} = [v \quad \alpha \quad \beta]^T$.

Reformulate the state-space equation as follows

$$\begin{bmatrix} \dot{\mathbf{x}} \\ \dot{\mathbf{z}} \end{bmatrix} = \begin{bmatrix} \mathbf{A}_{xx}(\mathbf{p}) & \mathbf{A}_{xz}(\mathbf{p}) \\ \mathbf{A}_{zx}(\mathbf{p}) & \mathbf{A}_{zz}(\mathbf{p}) \end{bmatrix} \begin{bmatrix} \mathbf{x} \\ \mathbf{z} \end{bmatrix} + \begin{bmatrix} \mathbf{B}_x(\mathbf{p}) \\ \mathbf{B}_z(\mathbf{p}) \end{bmatrix} \mathbf{u} + \begin{bmatrix} \mathbf{f}_{0x}(\mathbf{p}) \\ \mathbf{f}_{0z}(\mathbf{p}) \end{bmatrix}. \tag{8}$$

Note this state-space equation is divided into two parts concerning $\mathbf{x}$ and $\mathbf{z}$. $\mathbf{A}_{xx}(\mathbf{p})$, $\mathbf{A}_{xz}(\mathbf{p})$, $\mathbf{A}_{zx}(\mathbf{p})$ and $\mathbf{A}_{zz}(\mathbf{p})$ are the state transition matrixes. $\mathbf{B}_x(\mathbf{p})$ and $\mathbf{B}_z(\mathbf{p})$ are the input matrixes. $\mathbf{f}_{0x}(\mathbf{p})$ and $\mathbf{f}_{0z}(\mathbf{p})$ are offset terms. In this paper, the angular rate vector $\mathbf{x}$ is chosen as the controlled states, while signal $\mathbf{z}$ which is related to angular rates is treated as measurable disturbances[11]. Finally, the polytopic LPV model with the angular rates as the state is formed as:

$$\dot{\mathbf{x}} = \mathbf{A}_{xx}(\mathbf{p})\mathbf{x} + \mathbf{A}_{xz}(\mathbf{p})\mathbf{z} + \mathbf{B}_x(\mathbf{p})\mathbf{u} + \mathbf{f}_{0x}(\mathbf{p}). \tag{9}$$

For the convenience of discussion, (9) is rewritten as

$$\dot{\mathbf{x}} = \mathbf{A}(\mathbf{p})\mathbf{x} + \mathbf{H}(\mathbf{p})\mathbf{z} + \mathbf{B}(\mathbf{p})\mathbf{u} + \mathbf{f}_0(\mathbf{p}). \tag{10}$$

In the following, we consider the left wing tip loss damage of the GTM specifically, i.e. $l = 1$. A reasonable range of $\mathbf{p} \in [0, 1/3]$ is assumed over $\mathbf{p}$, to make sure the resulting damaged aircraft model is still physically controllable. In the range concerned, the damage severity is divided into 10 intervals, then the HOSVD method is used and the following singular values are obtained [11] as $\boldsymbol{\sigma} = [166.4366 \quad 0.1842 \quad 0.0035 \quad 0.0034 \quad \cdots]$.

Retaining the two larger singular values can effectively reduce the 10 vertexes to a polytopic model with 3 vertexes as,

$$\mathbf{S}(\mathbf{p}) \approx \mathcal{S}^* \bigotimes_{i=1}^{1} \boldsymbol{\omega}_i^*(\mathbf{p}) = \sum_{i_1=1}^{3} \boldsymbol{\omega}_{1,i_1}^*(\mathbf{p})\mathbf{S}_{i_1}^*. \tag{11}$$

Where $\mathbf{S}_{i_1}^*$ is the i_1^{th} vertex of the reduced model. By replacing the weight $\boldsymbol{\omega}$ of the reduced model with $\boldsymbol{\alpha}$, the LPV model can be written as

$$\Delta\dot{\mathbf{x}} = \sum_{i=1}^{3} \boldsymbol{\alpha}_i(\mathbf{p})(\mathbf{A}_i^*\Delta\mathbf{x} + \mathbf{H}_i^*\Delta\mathbf{z}) + \mathbf{B}(\mathbf{p})\Delta\mathbf{u} + \mathbf{f}_0(\mathbf{p}), \tag{12}$$

where $\mathbf{f}_0(\mathbf{p})$ is to compensate the deviation caused by the uncertainties in the operating point and disturbances.

The input matrix $\mathbf{B}(\mathbf{p})$, which is assumed fixed in [11], changes with damage severity as well. Although certain characteristics of $\mathbf{B}$, like the domination and signs of the diagonal elements, remain unchanged, we should take the changes in the elements of $\mathbf{B}$ into consideration. From the control law, the input matrix $\mathbf{B}(\mathbf{p})$ should be invertible and positive definite. To be more realistic, the input matrix $\mathbf{B}(\mathbf{p})$ is approximately expressed as the product of the damage-free input matrix and a adaptive diagonal matrix $\mathbf{\Lambda}$.

The damage-free matrix is

$$\mathbf{B}_{0\%} = \begin{bmatrix} -43.2662 & 0 & 0 \\ 0 & 39.5686 & 11.1409 \\ 0 & 3.2818 & -28.5370 \end{bmatrix},$$

and the input matrix of the 33% damage severity becomes

$$\mathbf{B}_{33\%} = \begin{bmatrix} -43.3142 & 2.6631 & -0.0442 \\ 0.6455 & 22.0466 & 11.3155 \\ 0.0211 & 1.8451 & -28.7231 \end{bmatrix},$$

By comparing the input matrixes of the damage-free and the 33% damage cases, the each column of $\mathbf{B}_{33\%}$ is changed to make it's diagonal elements equal to those of $\mathbf{B}_{0\%}$. Then the resulting matrix becomes

$$\mathbf{B}_{33\%}\mathbf{\Lambda}^{-1} = \begin{bmatrix} -43.2662 & 4.7796 & -0.0440 \\ 0.6448 & 39.5689 & 11.2422 \\ 0.0211 & 3.3115 & -28.5370 \end{bmatrix},$$

and,

$$\mathbf{\Lambda}^{-1} = \begin{bmatrix} 0.9989 & 0 & 0 \\ 0 & 1.7948 & 0 \\ 0 & 0 & 0.9935 \end{bmatrix},$$

where $\mathbf{\Lambda}^{-1}$ is a diagonal matrix. It is clear through this column transformation, the input matrix after the damage occurs can be approximated by the product of the damage-free input matrix $\mathbf{B}_{0\%}$ and a diagonal matrix $\mathbf{\Lambda}$, which is to be identified on line,i.e.

$$\mathbf{B}(\mathbf{p}) \approx \mathbf{B}\mathbf{\Lambda}^{-1}. \tag{13}$$

For clarity, $\mathbf{B}_{0\%}$ is written as $\mathbf{B}$. From above, it is sufficient that the elements of $\mathbf{\Lambda}$ satisfies the following inequality

$$1/3 \leq \mathbf{\Lambda}_{ii} \leq 2, \quad i \in \{1,2,3\}, \tag{14}$$

to represent all damage cases within the range of $\mathbf{p}$.

The GTM model can then be written as follows,

$$\Delta\dot{\mathbf{x}} = \sum_{i=1}^{3} \boldsymbol{\alpha}_i(\mathbf{p})(\mathbf{A}_i^*\Delta\mathbf{x} + \mathbf{H}_i^*\Delta\mathbf{z}) + \mathbf{B}\mathbf{\Lambda}^{-1}\Delta\mathbf{u} + \mathbf{f}_0, \tag{15}$$

$$\mathbf{y} = \mathbf{x}. \tag{16}$$

3 The LPV-MRAC Method

3.1 Controller Structure

The proposed LPV-MRAC method is structured as in Fig. 1.

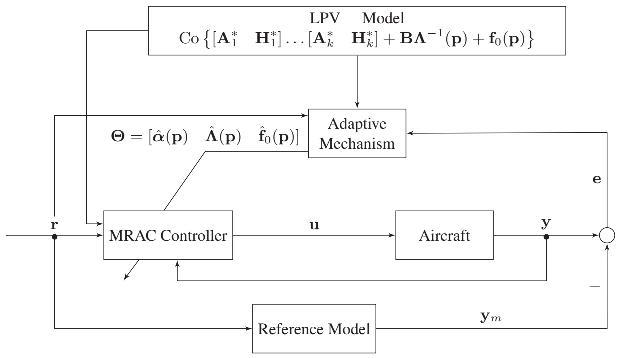

Fig. 1: Structure of the LPV-MRAC method

In Fig. 1, the controller is designed with state feedback and feedforward of the reference input $\mathbf{r}$. Parameters, including the interpolation coefficients $\hat{\boldsymbol{\alpha}}(\mathbf{p})$, the offset term $\hat{\mathbf{f}}_0$ and the uncertainty of the input matrix $\hat{\mathbf{\Lambda}}$, are adjusted by an adaptive mechanism which is driven by the reference input signals and the error between the controlled states and the reference states. The goal of the controller is to make the error $\mathbf{e}$ to be zero, and keep the desired performance after damage.

In this paper, the application of polytopic LPV models can reduce the number of identifying parameters, because using LPV models only needs identifying interpolation coefficients $\boldsymbol{\alpha}$, the uncertainty of input matrix $\mathbf{\Lambda}$ and offset terms $\mathbf{f}_0$ instead of identifying all adaptive parameters based on the states. Polytopic LPV models are good enough to reduce the computation cost for identifying the damaged model to improve damaged aircraft's transient performance. What's more, the HOSVD method can be extended to other damage cases. For example if the case of vertical-tail loss is added to the original problem, we can cope with it using the HOSVD method by increasing the dimension of the tensor to get the polytopic LPV model.

3.2 The LPV-MRAC Design

Fig. 1 adopts a model reference adaptive control structure with state feedback to recover the control performance and flight quality after damage. The reference model is as follows:

$$\dot{\mathbf{x}}_m = \mathbf{A}_m\mathbf{x}_m + \mathbf{B}_m\mathbf{r}, \tag{17}$$

$$\mathbf{y}_m = \mathbf{x}_m, \tag{18}$$

where the state matrix $\mathbf{A}_m$ and the input matrix $\mathbf{B}_m$ represent the desired dynamic performance. Since the derivative of the three angular rates $[p \quad q \quad r]$ can be affected by the three control surfaces directly, the input matrix $\mathbf{B}$ is square and invertible. In this way, we can rewrite the closed-loop system model as follows:

$$\begin{aligned}\dot{\mathbf{x}} =& \mathbf{A}_m\mathbf{x} + \mathbf{B}\mathbf{\Lambda}^{-1}\left[\mathbf{u} + \mathbf{\Lambda}[\mathbf{B}^{-1}(\mathbf{A}(\mathbf{p}) - \mathbf{A}_m)\mathbf{x}\right. \\ &\left. + \mathbf{B}^{-1}\mathbf{H}(\mathbf{p})\mathbf{z}] + \mathbf{\Lambda}\mathbf{B}^{-1}\mathbf{f}\right].\end{aligned} \tag{19}$$

Define $\boldsymbol{\mu}_i \triangleq [\mathbf{B}^{-1}(\mathbf{A}_i^* - \mathbf{A}_m) \quad \mathbf{B}^{-1}\mathbf{H}_i^*][\mathbf{x} \quad \mathbf{z}]^T$, and $\bar{\mathbf{f}}_0 \triangleq \mathbf{\Lambda}\mathbf{B}^{-1}\mathbf{f}_0$, then the closed-loop system model can then be reformulated as

$$\begin{aligned}\dot{\mathbf{x}} &= \mathbf{A}_m\mathbf{x} + \mathbf{B}\boldsymbol{\Lambda}^{-1}[\mathbf{u} + \boldsymbol{\Lambda}\sum_{i=1}^{3}\boldsymbol{\alpha}_i\boldsymbol{\mu}_i + \bar{\mathbf{f}}_0] \\ &= \mathbf{A}_m\mathbf{x} + \mathbf{B}\boldsymbol{\Lambda}^{-1}[\mathbf{u} + \boldsymbol{\Lambda}(\boldsymbol{\mu}_1 + \mathbf{M}\bar{\boldsymbol{\alpha}}) + \bar{\mathbf{f}}_0], \end{aligned} \tag{20}$$

where $\sum_{i=1}^{3}\boldsymbol{\alpha}_i(\mathbf{p}) = 1$, $\mathbf{M} \triangleq [\boldsymbol{\mu}_2 - \boldsymbol{\mu}_1 \quad \boldsymbol{\mu}_3 - \boldsymbol{\mu}_1]$, and $\bar{\boldsymbol{\alpha}} \triangleq [\boldsymbol{\alpha}_2 \quad \boldsymbol{\alpha}_3]$.

If all the parameters are known, then the control law would be (21) in order to match the reference model. Since the unknown parameters are estimated, the control law should be formed with the estimated parameters as (22).

$$\mathbf{u} = \boldsymbol{\Lambda}[\mathbf{B}^{-1}\mathbf{B}_m\mathbf{r} - \boldsymbol{\mu}_1 - \mathbf{M}\bar{\boldsymbol{\alpha}}] - \bar{\mathbf{f}}_0, \tag{21}$$

$$\mathbf{u} = \widehat{\boldsymbol{\Lambda}}[\mathbf{B}^{-1}\mathbf{B}_m\mathbf{r} - \boldsymbol{\mu}_1 - \mathbf{M}\hat{\bar{\boldsymbol{\alpha}}}] - \hat{\bar{\mathbf{f}}}_0, \tag{22}$$

where $\hat{\bar{\boldsymbol{\alpha}}}$ and $\hat{\bar{\mathbf{f}}}_0$ are the estimations of $\bar{\boldsymbol{\alpha}}$ and $\bar{\mathbf{f}}_0$ by the adaptive laws, respectively. Now given the definition of parameter errors as $\tilde{\bar{\boldsymbol{\alpha}}} \triangleq \hat{\bar{\alpha}} - \bar{\boldsymbol{\alpha}}$, $\tilde{\bar{\mathbf{f}}}_0 \triangleq \hat{\bar{\mathbf{f}}}_0 - \bar{\mathbf{f}}_0$, and $\tilde{\boldsymbol{\Lambda}} \triangleq \hat{\boldsymbol{\Lambda}} - \boldsymbol{\Lambda}$ and by substituting the control law (22) into (20), we have

$$\begin{aligned}\dot{\mathbf{x}} =& \mathbf{A}_m\mathbf{x} + \mathbf{B}\boldsymbol{\Lambda}^{-1}[\hat{\boldsymbol{\Lambda}}\mathbf{B}^{-1}\mathbf{B}_m\mathbf{r} - \tilde{\boldsymbol{\Lambda}}(\boldsymbol{\mu}_1 + \mathbf{M}\hat{\bar{\boldsymbol{\alpha}}}) - \hat{\bar{\mathbf{f}}}_0] \\ &- \mathbf{B}\mathbf{M}\tilde{\bar{\boldsymbol{\alpha}}}. \end{aligned} \tag{23}$$

The dynamics of the tracking error, which is defined as $\mathbf{e} \triangleq \mathbf{y} - \mathbf{y}_m = \mathbf{x} - \mathbf{x}_m$, can then be formed as,

$$\begin{aligned}\dot{\mathbf{e}} =& \mathbf{A}_m\mathbf{e} + \mathbf{B}\mathrm{diag}(\mathbf{B}^{-1}\mathbf{B}_m\mathbf{r} - \boldsymbol{\mu}_1 - \mathbf{M}\tilde{\bar{\boldsymbol{\alpha}}})\boldsymbol{\Lambda}^{-1}\tilde{\boldsymbol{\lambda}}_d \\ &- \mathbf{B}\boldsymbol{\Lambda}^{-1}\tilde{\bar{\mathbf{f}}}_0 - \mathbf{B}\mathbf{M}\tilde{\bar{\boldsymbol{\alpha}}}, \end{aligned} \tag{24}$$

where $\tilde{\boldsymbol{\lambda}}_d$ is a column vector consisting the diagonal elements of $\tilde{\boldsymbol{\Lambda}}$.

It is well known that for a given symmetric positive definite matrix $\mathbf{Q}$, there exists a symmetric positive definite matrix $\mathbf{P}$ satisfying $\mathbf{A}_m^T\mathbf{P} + \mathbf{P}\mathbf{A}_m + \mathbf{Q} = \mathbf{0}$. The adaptive laws for the controller (22) are designed using the Lyapunov stability criterion [14], and the Lyapunov function is chosen to be

$$V(\mathbf{e}) = \mathbf{e}^T\mathbf{P}\mathbf{e} + \tilde{\boldsymbol{\lambda}}_d^T\boldsymbol{\Gamma}_v^{-1}\boldsymbol{\Lambda}^{-1}\tilde{\boldsymbol{\lambda}}_d + \tilde{\bar{\mathbf{f}}}_0^T\boldsymbol{\Gamma}_f^{-1}\boldsymbol{\Lambda}^{-1}\tilde{\bar{\mathbf{f}}}_0 + \tilde{\bar{\boldsymbol{\alpha}}}^T\boldsymbol{\Gamma}_\alpha^{-1}\tilde{\bar{\boldsymbol{\alpha}}}. \tag{25}$$

Where $\boldsymbol{\Gamma}_v$, $\boldsymbol{\Gamma}_f$, and $\boldsymbol{\Gamma}_\alpha$ are symmetric positive-definite matrices. The derivative of the Lyapunov function V is

$$\begin{aligned}\dot{V} &= \dot{\mathbf{e}}^T\mathbf{P}\mathbf{e} + \dot{\tilde{\boldsymbol{\lambda}}}_d^T\boldsymbol{\Gamma}_v^{-1}\boldsymbol{\Lambda}^{-1}\tilde{\boldsymbol{\lambda}}_d + \dot{\tilde{\bar{\mathbf{f}}}}_0^T\boldsymbol{\Gamma}_f^{-1}\boldsymbol{\Lambda}^{-1}\tilde{\bar{\mathbf{f}}}_0 + \dot{\tilde{\bar{\boldsymbol{\alpha}}}}^T\boldsymbol{\Gamma}_\alpha^{-1}\tilde{\bar{\boldsymbol{\alpha}}} \\ &= -\mathbf{e}^T\mathbf{Q}\mathbf{e} - 2[\mathbf{e}^T\mathbf{P}\mathbf{B}\mathbf{M} - \dot{\tilde{\bar{\boldsymbol{\alpha}}}}^T\boldsymbol{\Gamma}_\alpha^{-1}]\tilde{\bar{\boldsymbol{\alpha}}} \\ &+ 2[\mathbf{e}^T\mathbf{P}\mathbf{B}\mathrm{diag}(\mathbf{B}^{-1}\mathbf{B}_m\mathbf{r} - \boldsymbol{\mu}_1 - \mathbf{M}\tilde{\bar{\boldsymbol{\alpha}}}) + \dot{\tilde{\boldsymbol{\lambda}}}_d^T]\boldsymbol{\Lambda}^{-1}\tilde{\boldsymbol{\lambda}}_d \\ &- 2[\mathbf{e}^T\mathbf{P}\mathbf{B} - \dot{\tilde{\bar{\mathbf{f}}}}_0\boldsymbol{\Gamma}_f^{-1}]\boldsymbol{\Lambda}^{-1}\tilde{\bar{\mathbf{f}}}. \end{aligned} \tag{26}$$

If the adaptive laws are chosen as follows

$$\begin{aligned}\dot{\tilde{\boldsymbol{\lambda}}}_d &= -\boldsymbol{\Gamma}_v\mathrm{diag}(\mathbf{B}^{-1}\mathbf{B}_m\mathbf{r} - \boldsymbol{\mu}_1 - \mathbf{M}\tilde{\bar{\boldsymbol{\alpha}}})(\mathbf{P}\mathbf{B})^T\mathbf{e} \\ \dot{\tilde{\bar{\mathbf{f}}}}_0 &= \boldsymbol{\Gamma}_f(\mathbf{P}\mathbf{B})^T\mathbf{e} \\ \dot{\tilde{\bar{\boldsymbol{\alpha}}}} &= \boldsymbol{\Gamma}_\alpha\mathbf{M}^T(\mathbf{P}\mathbf{B})^T\mathbf{e}, \end{aligned} \tag{27}$$

then $\dot{V} = -\mathbf{e}^T\mathbf{Q}\mathbf{e}$, namely the derivative of the Lyapunov function V is negative unless $\mathbf{e} = 0$. The design process of the control law and adaptive law in this paper is quite similar to the classical ones using the Lyapunov method. The stability and asymptotic error convergence can also be proved using the same procedures. Based on Barbalat's lemma [15], the state error $\mathbf{e} = \mathbf{y} - \mathbf{y}_m$ goes to zero asymptotically. And we can also know that the obtained adaptive laws (27) guarantee that the error approaches to zero, but it can't be asserted that the parameters, $\dot{\tilde{\boldsymbol{\lambda}}}_d$, $\dot{\tilde{\bar{\mathbf{f}}}}_0$, and $\dot{\tilde{\bar{\boldsymbol{\alpha}}}}$, converge to their true values.

4 Case Study

4.1 Simulation of the LPV-MRAC method

In this section, the proposed LPV-MRAC method is tested on the GTM simulation model with left wing tip loss damage. The GTM is a 5.5% dynamically scaled twin-turbine powered aircraft model, and designed and manufactured in the NASA AvSP program.The simulation model is a nonlinear MATLAB/SIMULINK model which includes several adverse conditions, such as large angle of attack, coupling between lateral and longitudinal dynamics, etc.

The design procedure follows from the descriptions in sections 2 and 3, i.e. 10 damages severities in the left wing tip damage conditions are used to design the LPV model of the damaged aircraft, and then the HOSVD method is used to reduce the number of polytopic vertexes without reducing much accuracy. Further more, the design of LPV-MRAC controller and adaptive laws is quite similar to the classical ones using the Lyapunov method.

Simulation is conducted on the 6DOF nonlinear GTM model, and the maximum deflecting angles of the control surfaces are 40 degrees. Before damage, the nonlinear model is trimmed at the operating point with $V = 46.3m/s$, $H = 304.8m$, $\alpha = 4.096rad$, and the other states are zero. Further more, 20% loss of the left wing tip is injected to the simulated nominal aircraft to validate this direct adaptive control method.

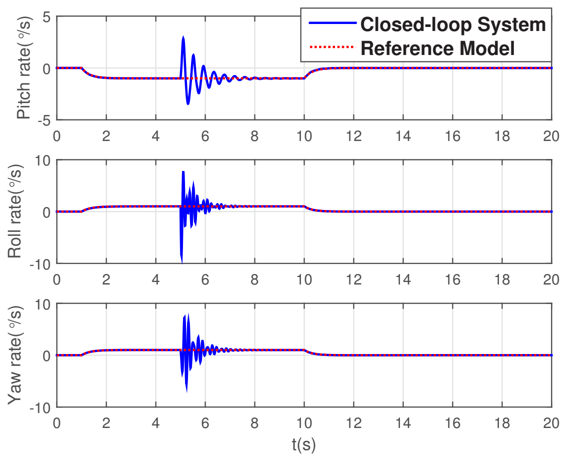

Fig. 2: Angular rate responses of the closed-loop system and the reference model

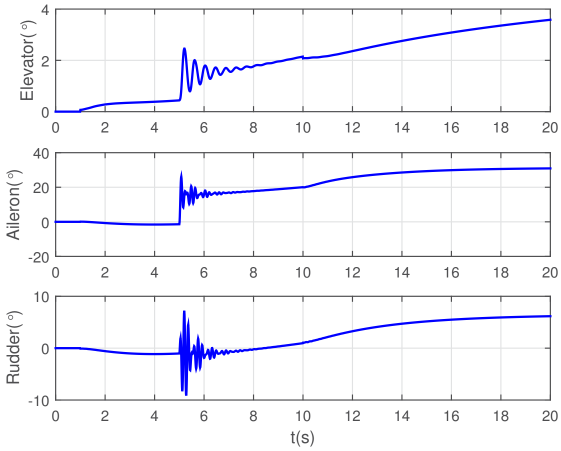

Fig. 3: Control surface deflections

The reference input $\mathbf{r}$ starts with 0, and at 1s the value $[-1 \quad 1 \quad 1]$ is applied. Fig. 2 shows the angular rates track the reference model's states perfectly from 0 to 5 seconds. At 5s, abrupt left wing tip damage is injected to the model, then the angular rates become stable after a transient oscillation period of about 3 seconds. This benefits from the simple calculation of the polytopic LPV models and the introduction of the input matrix $\mathbf{B}$'s uncertainty, namely $\mathbf{\Lambda}$.

From Fig. 3, it can be seen that the control surfaces are not saturated, so the angular rates of the closed-loop system can still be controlled from a physics point of view. It can also be seen that the deflection of the aileron, which is used to compensate the effect of the wing tip damage, is the largest of all.

Fig. 4 shows that the interpolation coefficients $\boldsymbol{\alpha}_i$, the external disturbance terms $\mathbf{f}_i$ adjust rapidly and reach relatively stable values. The sum of the interpolation coefficients also satisfies (4). In this paper, uncertainty over the input matrix is represented by the diagonal matrix $\mathbf{\Lambda}$, whose values are shown in Fig. 4. Fig. 4 also shows that the variations of $\mathbf{\Lambda}_{ii}$ are within the inequality constraints (14).

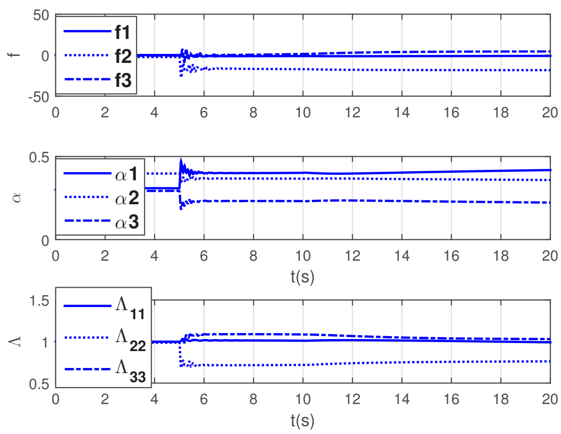

Fig. 4: Adaptive parameters, $\boldsymbol{\alpha}$, $\mathbf{f}$ and $\mathbf{\Lambda}$

4.2 Simulation with Gaussian Measurement Noise

In this section, white Gaussian measurement noises with zero mean and variance of $[0.1 \quad 0.001 \quad 0.005 \quad 0.01 \quad 0.1 \quad 0.01 \quad 0.005 \quad 0.005 \quad 0.01 \quad 0.01 \quad 0.1 \quad 0.1]$ are added to the state variables to verify the proposed LPV-MRAC method under a more realistic condition. This variance vector corresponds to a state sequence of airspeed, angle of attack, pitch rate, pitch angle, altitude, sideslip angle, roll rate, yaw rate, yaw angle, roll angle, x location and y location in the aircraft body coordinate system. Simulation results are shown in Fig. 5 to Fig. 7.

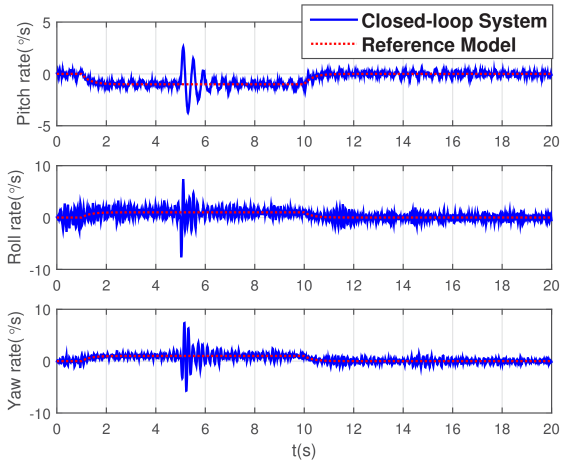

Fig. 5: Commands and angular rate responses under Gaussian measurement noises

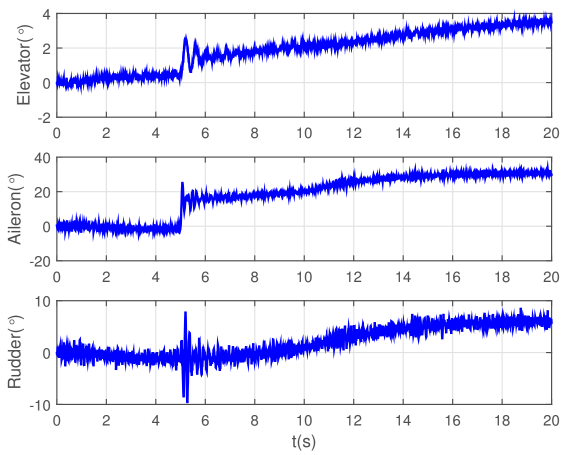

Fig. 6: Control surface deflections under Gaussian measurement noises

It can be seen from Fig. 5 to Fig. 7 that the simulation results under Gaussian measurement noises are similar to those without measurement noises. Further more, the simulation results under Gaussian measurement noises demonstrate the applicability of this proposed LPV-MRAC method.

4.3 Flight Quality Evaluation

In this subsection, the C-star response criterion is used for flight quality evaluation. C-star response criterion is combination of aircraft's pitch rate and normal overload formed as follows $C^* = n_z + \frac{V_{co}}{g}q$, where V_{co} is the cross speed, whose value commonly used is 122 m/s, n_z is the normal overload, and q represents the pitch rate.

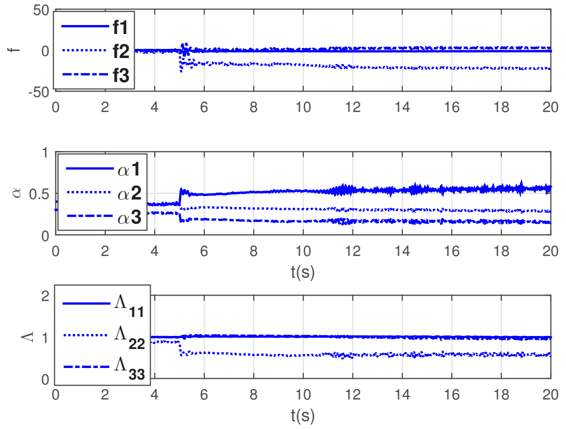

Fig. 7: Adaptive parameters $\boldsymbol{\alpha}$, $\mathbf{f}$ and $\boldsymbol{\Lambda}$ under Gaussian measurement noises

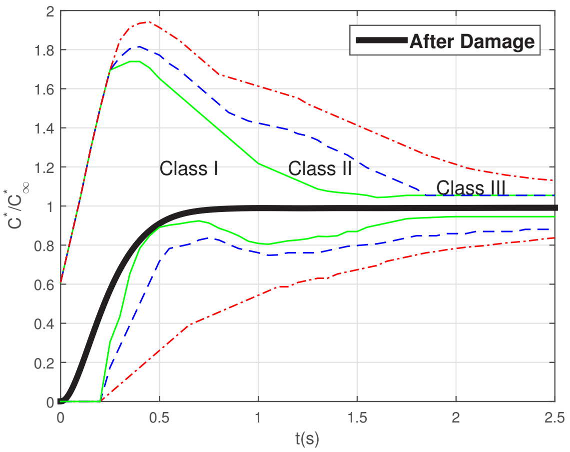

Fig. 8: C^* response criterion after the damage

The C-star controller is a longitudinal controller, so the output of the C-star controller u_c is passed to the first element in the reference input signals $\mathbf{r}$. A PI controller is chosen as the outer-loop C-star controller, and its form is as follows, $u_c = K_P e^* + K_I \int e^* dt$. Where $K_P = 5$, $K_I = 1$, and the error e^* is defined as the difference between aircraft's C-star response and the desired model's response, i.e. $e^* = C^* - C_m^*$. The transfer function of the desired longitudinal model is $G_m(s) = \frac{55}{s^2+13.5s+55}$. And C_m^* is the response of $G_m(s)$ with a unit step input.

In Fig. 8, flight quality evaluation is made after 10 seconds of damage happens when controller and states are stable after a transient process. The C-star response is still in Class I which indicates that the developed LPV-MRAC method is good enough to compensate the damages in the aircraft structure and parameters introduced by the damage to keep the flight quality.

5 Conclusions

Structural damage represents a severe case in which aircraft flight quality and flight safety deteriorate significantly, posing challenges to flight control systems design. This paper proposed an LPV-MRAC method with the introduction of uncertainty of input matrix $\mathbf{B}$. The proposed controller is validated on the GTM simulation model with left wing tip loss by simulation. Simulation results show that this developed LPV-MRAC method can reduce computational cost of identifying the damaged aircraft model, and recover flight quality after damage. Further research for improving flight performance of aircraft with structural damages could be carried out.

6 Acknowledgements

We have benefited from the flight quality evaluation software from the Laboratory of Flight Control and Mission Decision of Beihang University.

References

[1] J.X. Guo, G. Tao, Multivariable Adaptive Control of NASA Genetic Transport Aircraft Model with Damage, *Journal of Guidance, Control, and Dynamics*, September-October 2011.

[2] B. Gotz, M. Mark, M. Steven, Piloting Strategies for Controlling a Transport Aircraft after Vertical-tail Loss, *Journal of Aircraft*, January-February 2006.

[3] C.M. Belcastro, J.V.Foster, Aircraft loss-of-cotrol accident analysis, *AIAA trans. Guidance, Navigation,and Control Conference*, Toronto, Canada, August 2010.

[4] N. Nguyen, K. Krishnakumar, J. Kaneshige, Dynamics and Adaptive Control for Stability Recovery of Damaged Asymmetric Aircraft, *AIAA Guidance, Navigation, and Control Conference and Exhibit*, Keystone, Colorado, August 2006.

[5] N. Nguyen, K. Krishnakumar, J. Kaneshige, Flight Dynamics and Hybrid Adaptive Control of Damaged Aircraft, *Journal of Guidance, Control, and Dynamics*, May-June 2008.

[6] M. Santillo, M. Holzel, Adaptive Control of the NASA Generic Transport Model Using Retrospective Cost Optimazation, *AIAA . Guidance, Navigation, and Control Conference*, Chicago, lllinois, August 2009.

[7] C. Cao, N. Hovakimyan, Design and Analysis of a Novel $\mathcal{L}_1$ Adaptive Controller,Part I : Control Signal and Asymptotic Stability, *American Control Conference*, Minnesota, USA, June 2006.

[8] C. Cao, N. Hovakimyan, Design and Analysis of a Novel $\mathcal{L}_1$ Adaptive Controller,Part II : Guaranteed Transient Performance, *American Control Conference*, Minnesota, USA, June 2006.

[9] I. Gregory, C. Cao, Flight Test of an $\mathcal{L}_1$ Adaptive Controller Design for NASA AirSTAR Flight Test Vehicle, *AIAA. Guidance, Navigation, and Control Conference*, Toronto, Canada. August 2010.

[10] Y. Tansel, J. Anthony, Derivative-Free Model Reference Adaptive Control, *Journal of Guidance, Control, and Dynamics*, July-August 2011.

[11] X. Xu, L. Yang, J. Zhang, MRAC Control with Prior Model Knowledge for Asymmetric Damaged Aircraft, *The Scientific World Journal*, Noverber 2014.

[12] C. Tseng, B. Chen, H. Uang, Fuzzy Tracking Control Design for Nonlinear Dynamic System via T-S Fuzzy Model, *IEEE TRANSACTION ON FUZZY SYSTEMS*, June 2001.

[13] P. Baranyi, TP model transformation as a way to LMI-based controller design, *AIAA trans. Industrial Electronics*, April 2004.

[14] P.A. Ioannou, J. Sun, Robust Adaptive Control, Mineola, New York: Dover Publication, 1995:834.

[15] K.J. Astrom, B. Wittenmark, Adaptive Control: Model Reference Adaptive System, Beijing: Science Press, 2003:205.